

## **Chapter 4: Development of a high particle loading novel Cu ink for the fabrication of a three-dimensional hierarchical porous structure**

---

This chapter is dedicated to the development and characterization of an innovative *Cu* ink formulation with a high *Cu* content exceeding 95 weight percent (*wt%*). The research aims to establish an economically viable approach by employing PLA as the binder material and dichloromethane as the solvent within the binder-solvent system. A detailed and systematic investigation has been conducted to examine the impact of varying filler and binder content on the rheological properties of the ink. These properties include critical parameters such as viscosity and shear thinning behavior, which are essential for evaluating the suitability of the ink for DIW processes.

The study delves deeply into the relationship between the composition of the ink and its rheological performance. By analyzing these factors, insights into the optimization of ink formulations for advanced manufacturing techniques can be gained. The Herschel-Bulkley model has been employed to provide a comprehensive understanding of the rheological behavior of the ink. This modelling approach allows for the establishment of a quantitative framework to describe how the ink responds to varying shear rates, providing a valuable tool for predicting performance in practical applications.

To validate the practical efficacy of the developed high-performance *Cu* ink, an HP-*Cu* sample has been fabricated using the DIW process. This final stage serves as a robust demonstration of the developed ink's capability to produce high-quality components suitable for various applications. The results of this comprehensive study highlight the

potential of the novel *Cu* ink formulation as a cost-effective and efficient material for additive manufacturing technologies.

## 4.1 Results and discussions

### 4.1.1 Development of High particle loaded *Cu* ink

The first step is the development of an optimum ink. Hence, to achieve the same, five different combinations of ink with *Cu* particle loading as 91 wt %, 93 wt %, 95 wt%, 97 wt% and 99 wt % were developed. The *Cu* inks were prepared with different compositions of the binder, and the rheological characterization was performed. All the inks were showing the shear thinning behaviour. To date, a maximum of 95 wt % of *Cu* loading has been achieved for DIW. However, previous studies have shown that high particle loading in 3D printable ink results in a higher storage modulus of inks. High storage modulus allows better control in retaining the shape of extruded ink thereby promoting the printing of finer and more complex shapes. However, difficulty in the extrusion of high particle-loading ink through the micro nozzle restricts the upper limit of particle loading that can be achieved. Thus, to explore the possibility of high particle loading, 97 wt% and 99 wt%*Cu* inks were also developed and tested. The green *Cu* parts were fabricated successfully using the *Cu* ink with particle loading of 93 wt%, 95 wt% and 97 wt%, respectively. However, the *Cu* ink with particle loading 91 wt % exhibited poor printability with the green parts getting collapsed. The poor printability of 91 wt% *Cu* ink could be attributed to the low amount of *Cu* content which causes the reduction in the viscosity of the ink and improper bonding between the copper particles. The rheological characterization shown in Fig. 4.1 reveals that the viscosity of 91 wt% and 97 wt% ink was 220 Pa-s and 5500 Pa-s, respectively, at  $0.1 \text{ s}^{-1}$  shear rate. Hence, low viscosity in 91 wt% *Cu* ink is the major cause of its poor

printability. Moreover, no printing of the *Cu* green part was achieved using 99 wt% *Cu* ink owing to the clogging of the micro nozzle.

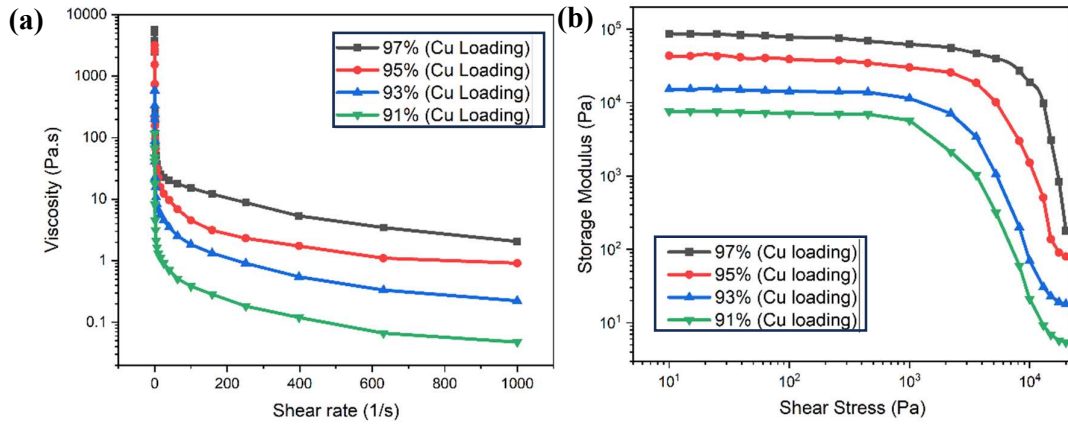


Fig. 4.1: Effect of particle loading on a) viscosity and b) storage modulus for the prepared *Cu* ink

Hence, amongst the combination of the *Cu* ink, the inks with particle loading 93 wt%, 95 wt%, and 97 wt% were found to be suitable. All three combinations exhibited an ideal shear thinning behavior and storage modulus values as required for the DIW process. However, in addition to the rheological properties, other process parameters such as print speed, nozzle size and layer thickness also significantly affect the printability of green *Cu* samples. Hence, based on the rheological properties, *Cu* inks with loading of 93 wt%, 95 wt % and 97 wt% have been selected for further process development.

#### 4.1.2 Rheological properties of *Cu* ink with variation of binder and filler content

The details regarding the rheological properties of the prepared *Cu* ink with different *Cu* and PLA loading are shown in Fig. 4.2.

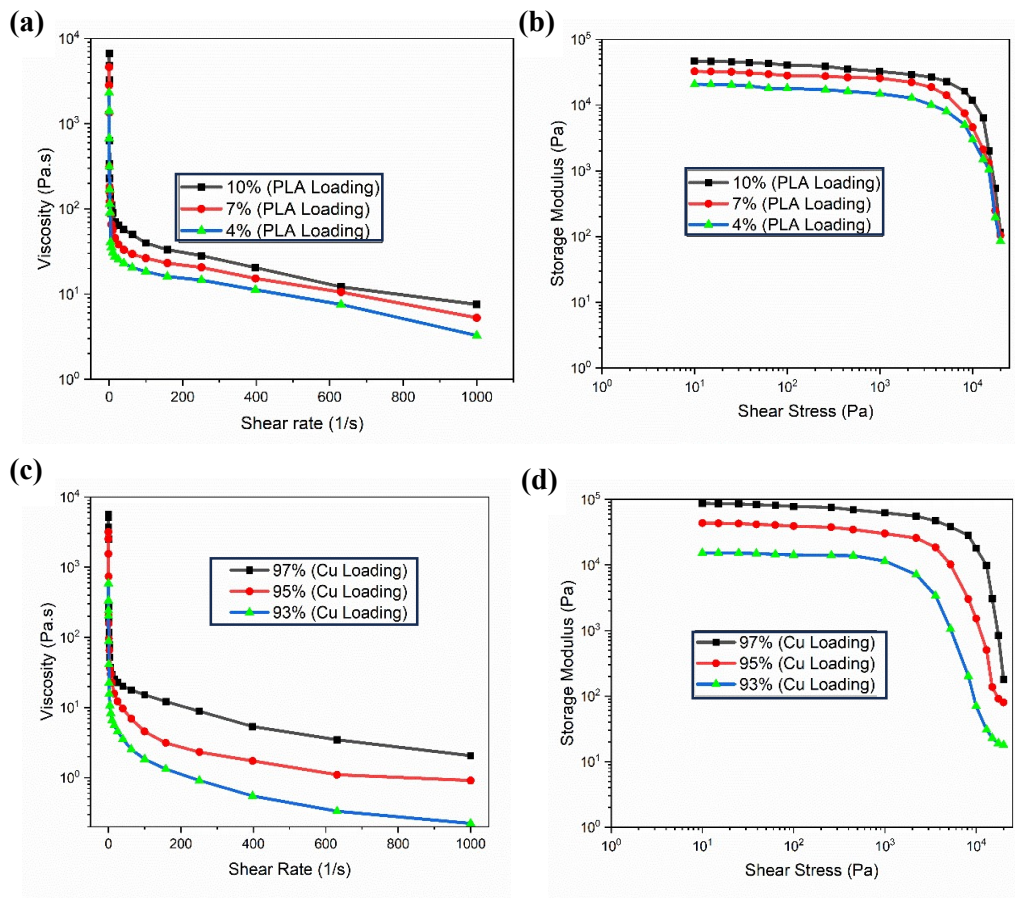


Fig. 4.2: Variation of a) Viscosity vs Shear rate for increased binder loading b) storage modulus vs shear stress for increased binder loading c) Viscosity vs Shear rate for increased *Cu* loading and d) Storage modulus vs shear stress for increased *Cu* loading

It could be inferred that as the amount of PLA binder was increased, the viscosity and storage modulus of the *Cu* ink also steadily increased, as illustrated in Fig. 4.2 (a) and (b). The reason for the increase in viscosity was an increase in the binding ability between the *Cu* particles and the PLA binder. Due to the increase in the binding ability, resistance to flow increases and hence more force is required to achieve the shear thinning behaviour. Moreover, the storage modulus of the *Cu* ink with the highest PLA content (10 wt%) was higher than ink with 4 wt% and 7 wt% PLA loading, which makes this ink qualify for printability. Our main objective was to minimize the binder content because as the binder content increases the strength will be reduced and higher porosity was observed at the

places where the binder content was higher. Therefore, for the subsequent characterization, the effect of the increase in the content of *Cu* particle loading keeping PLA constant was analyzed.

The effect of an increase in *Cu* loading on the prepared ink has been shown in Fig. 4.2 (c & d). It is evident that the rheological characteristics of the prepared inks are closely connected to the amount of variation in *Cu* loading. Moreover, with the increase in the shear rate, prepared inks with different *Cu* loading i.e. 93 wt%, 95 wt% and 97 wt%, respectively, exhibited the shear thinning behavior. For instance, when the shear rate was increased from 0.1 to 25 s<sup>-1</sup>, the viscosity of heavily loaded 97 wt% *Cu* loading ink got reduced from 5500 Pa-s to 584 Pa-s. This could be attributed to the variation in the entanglement of *Cu* particles at different values of shear rate. The *Cu* ink's particles were entangled with one another and exhibited a high viscosity at a very low shear rate or at rest. However, as the shear rate was increased, the *Cu* ink's particle entanglement diminished due to the shear stress experienced during the various flow stages, leading to shear thinning behavior. The observed shear thinning behavior in the prepared *Cu* ink is vital for DIW as it ensures a smooth flow of the ink through the nozzle without any clogging.

Similarly, at the same shear rates, the *Cu* ink with high solid loading exhibited higher viscosities than *Cu* ink with low solid loading. The viscosity of ink with 93 wt% *Cu* loading was approximately 480 Pa-s at 0.1 s<sup>-1</sup>, whereas the viscosity of the *Cu* ink with 97 wt% *Cu* loading reached to 5500 Pa-s when the shear rate was 0.1 s<sup>-1</sup>.

Hence, viscosity is a key parameter for achieving successful and precise DIW. It governs how the ink flows, adheres, and solidifies which ultimately determines the quality of the printed structures. Optimizing viscosity ensures smooth extrusion, accurate deposition, and stable printed features, making it a cornerstone of DIW process control. Another important factor for successful DIW is the ability of the extruded ink to retain its shape after extrusion

determined using storage modulus. The storage modulus measures the elastic behavior of the ink and its ability to resist deformation when a force is applied. At high value of storage modulus, ink behaves more like an elastic solid than a viscous fluid. It can recover its shape after deformation and resist flow under its own weight or external forces ensuring that printed structures maintain their geometry and do not collapse or spread after deposition. Whereas at low value of storage modulus renders poor shape retention which may lead to the collapse of printed features. The *Cu* ink exhibits a plateau in elastic modulus when the shear stress is below the shear yield stress ( $\tau_y$ ), indicating a linear viscoelastic behavior. In this region, the storage modulus remains constant. However, as the shear stress exceeds ( $\tau_y$ ), the value of storage modulus decreases significantly, marking the onset of irreversible plastic deformation. The storage modulus ( $G'$ ) of the prepared *Cu* ink with varying *Cu* loading has been shown in Fig. 4.2 (d). It was found that when the shear stress was less than the shear yield stress ( $\tau_y$ ), all the *Cu* inks with various solid contents exhibited a plateau in elastic modulus, thereby representing a linear viscoelastic characteristic. Moreover, as the shear stress value was increased, the storage modulus of the *Cu* ink remained almost constant in the linear viscoelastic region. However, a significant decrease in the shear elastic modulus from  $\tau_y$  of the *Cu* ink was observed indicating the start of irreversible plastic deformation. The *Cu* loaded ink with a 97% content had the highest equilibrium elastic modulus (about  $0.90 \times 10^5 Pa$ ) and shear yield stress (about  $0.5 \times 10^4 Pa$ ) of all the manufactured *Cu* inks. The linear viscoelastic region of *Cu* ink's elastic modulus ranged between  $10^4 Pa$  and  $10^5 Pa$  in magnitude according to Fig. 4.2 (d). Hence, it could be inferred that both the storage modulus and shear yield stress of the *Cu* ink increased with the increase in the amount of *Cu* loading. It has been reported in the previous studies [74] that high value of storage modulus signifies the *Cu* parts to retain its

shape which results in very thin and porous parts with high relative density. The storage modulus ( $G'$ ) of the prepared  $Cu$  ink, as shown in the Fig. 4.2, highlights this characteristic. The prepared  $Cu$  ink with high particle loading of 97 wt% was found to be stable with an equilibrium elastic modulus of approximately  $0.90 \times 10^5 Pa$  and a shear yield stress of about  $0.5 \times 10^4 Pa$ .

#### 4.1.3 Rheological Characterization of the optimized $Cu$ ink

The rheological properties of the prepared  $Cu$  ink illustrated in Fig. 4.3 (a) shows that the ink exhibits shear-thinning behavior with the increase in shear rate. This phenomenon arises from changes in the entanglement of  $Cu$  particles at different shear rates, the particles entangle or interact through forces like van der Waals interactions or hydrogen bonding. At low shear rates these interactions dominate, resulting in a higher viscosity as the fluid resists flow. However, at higher shear rates, the applied force overcomes these interactions, breaking them down and allowing the fluid components to move freely. Moreover, at higher shear rates, the time available for interactions between fluid components is reduced and less interaction time lowers the internal resistance to flow, reducing viscosity.

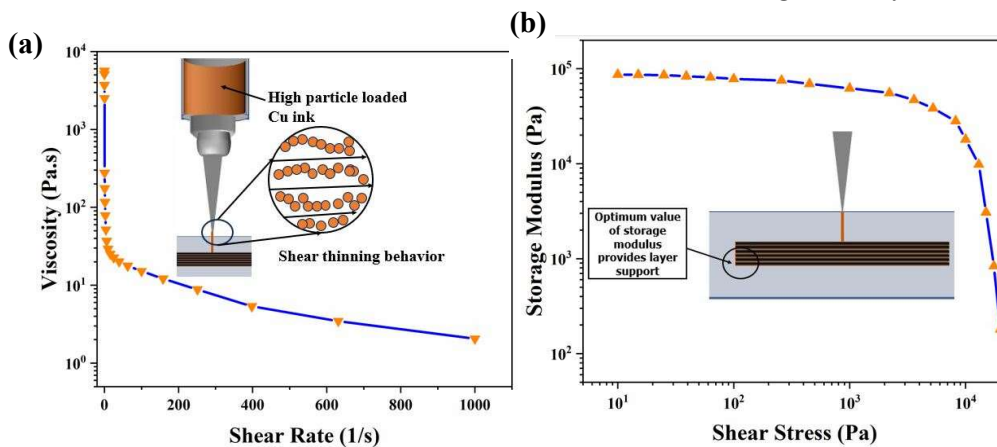


Fig. 4.3: a) Viscosity vs Shear rate b) storage modulus vs shear stress for the prepared  $Cu$  ink with 97 wt% particle loading

Fig. 4.3 (b) indicates that the linear viscoelastic range for the elastic modulus of the *Cu* ink spans from  $10^4 Pa$  and  $10^5 Pa$ . Previous studies [74] have suggested that a high storage modulus is essential for maintaining the shape of printed *Cu* components, enabling the production of thin, porous parts with high relative density. Thus, the fabricated *Cu* ink with extremely high particle loading (97 wt %) proved to be well-suited for the DIW of HP-*Cu* current collector.

Therefore, it could be established that the variation in *Cu* powder concentration was crucial in changing the viscosity of ink for DIW. High *Cu* loading in the prepared ink leads to higher viscosity thereby requiring higher force to flow. To further establish the observed behaviour, the results were validated using the Herschel-Bulkey equation, which typically describes the flow behaviour of inks that can be used for DIW. Equation (4.1) given below defines the Herschel-Bulkley (HB) model.

$$\tau = \tau_y + k\dot{\gamma}^n \dots\dots\dots (4.1)$$

Where  $n$  denotes the shear thinning exponent,  $k$  denotes the viscosity parameter,  $\dot{\gamma}$  denotes the shear rate,  $\tau_y$  denotes the yield stress, and  $\tau$  denotes the applied shear stress.

As per the HB model, the flow of the ink cannot take place if the values of stress are lower than yield stress  $\tau_y$ . The inference from this model is helpful in explaining the flow of inks and describes that ideal non-Newtonian fluids will not flow below a yield stress. Moreover, the HB model explains the concept of rate-dependent viscosity during the flow of the ink. Specifically, if the value of  $n < 1$ , the ink will exhibit a shear-thinning behavior also referred to as pseudo-plasticity, whereas a shear-thickening behavior will be observed for  $n > 1$ . This means that when the load on ink increases beyond the yield stress, the ink must exhibit a shear thinning behavior i.e. the ink will experience a drop in viscosity due to an increase in shear rate. The reason for this could be attributed to the attrition between

solid metal particles i.e. *Cu* in this case and additives. Hence, it could be established that as the shear stress reaches yield stress  $\tau_y$  value, the shear rate becomes zero, thereby allowing the *Cu* inks to flow.

**Table 4.1: Values of parameters obtained after fitting using HB equation**

<i>Cu</i> loading (wt%)	Shear thinning exponent, $n$	Value of $k$	$R^2$
97	0.54	7.11	0.990
95	0.69	5.89	0.988
93	0.81	4.58	0.991

Thereafter, as shear stress further increases beyond yield stress, it eventually attains a stable value as per the HB equation. With the aid of Fig. 4.4 the relation between shear rate & shear stress can be understood, which is in accordance with the general trend of Equation (4.1).

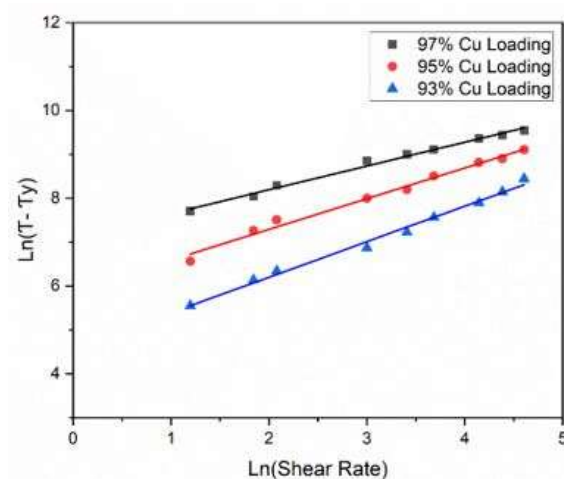


Fig. 4.4: Fitting curve for 93 wt%, 95 wt% & 97 wt% *Cu*-loaded inks with values of  $n = 0.81, 0.69, \text{ and } 0.54$

Thus, to promote proper extrusion and deposition of the ink in DIW, the value of  $n$  should be maintained as low as possible. Fig. 4.4 shows the fitting curve of the 93wt%, 95wt%, & 97wt% loaded *Cu* ink. Calculations were made for the shear thinning behaviour of the ink having the best rheological properties. It can be observed from Table 4.1 that the value of the slope is 0.81, 0.69, & 0.54, which means that the value of  $n$  is less than one for all the inks developed with different *Cu* loading. Amongst all the inks prepared, the *Cu* ink having 97 wt % exhibited the minimum value of  $n$ . Hence, it could be established that the *Cu* ink with 97 wt % loading is ideal for DIW.

According to earlier studies for DIW on colloidal ink, equation 4.2 can be used to determine whether *Cu* ink's elastic modulus is acceptable for DIW.

$$y = C \left( \frac{\phi}{\phi_{gel}} - 1 \right)^x \dots\dots\dots(4.2)$$

Where  $x$  refers to the scaling component ( $\sim 2.5$ ),  $y$  refers to the elastic property to be determined,  $\tau_y$  is the shear yield stress,  $\phi_{gel}$  refers to the gel point also known as critical volume fraction, and  $\phi$  refers to the colloid volume fraction. Colloidal ink's elastic properties are primarily influenced by two parameters:  $\phi_{gel}$ , which is inversely related to bond strength, and,  $\phi$  which is proportional to bond density. As shown in Fig. 4.5, the *Cu* green body fabricated using 93 wt% *Cu* ink was found to crumble and deform significantly. However, for the *Cu* ink with *Cu* loading as 95 wt% or higher, successful DIW of the green body was obtained. Thus, 95 wt% *Cu* loading has been assumed as a critical mass fraction. In order to achieve a suitable match with the model, the mass fraction of *Cu* inks were converted into the volume fraction. The corresponding *Cu* volume fractions of the 93 wt% *Cu*, 95 wt% *Cu* & 97 wt% *Cu* were found to be 65 vol%, 72 vol% and 83 vol% respectively. The storage modulus of the *Cu* ink with 97 wt% *Cu* loading was about  $0.90 \times 10^5 Pa$ , as shown in Fig. 4.2 d. The value of  $C$  in the present

work was found to be about  $0.98 \times 10^7$  and as per the colloidal ink model, the value of  $C$  in the range of  $10^7$  refers to the formation of strong gel, thereby indicating the good printability of the ink.

#### 4.1.4 DIW of green Cu parts

The ink with a  $Cu$  loading greater than 97 wt% was found to be unsuitable for DIW owing to the clogging of the nozzle. Moreover, ink with  $Cu$  loading less than 93 wt% was also found to be unsuitable due to decreased elastic modulus, significant deformation, and collapse defects. Thus, the DIW process was performed using the ink with  $Cu$  loading in the range of 93 wt% to 97 wt% as shown in Fig. 4.5. Since the storage modulus of 97 wt% loaded  $Cu$  ink was highest among the prepared inks, the ink with 97 wt%  $Cu$  loading has been selected as an optimum ink combination for further processing. Thus, it could be established from Fig. 4.5 that 97 wt%  $Cu$  loading ink exhibited good printability as compared to ink with 93 wt% and 95 wt%  $Cu$  loading. To establish the proof of concept for the above discussion, complex shape HP– $Cu$  structures were printed using the optimum ink as shown in Fig. 4.6. It could be observed clearly from Fig. 4.6 that the prepared optimum  $Cu$  ink was found to be suitable for the DIW of the HP- $Cu$  structures. Furthermore, to evaluate the printing quality of the prepared green  $Cu$  sample using optimum ink, the morphology of the ink and the green sample was analyzed as shown in Fig. 4.7.

It can be observed from Fig. 4.7 that all the  $Cu$  particles in the ink were wetted completely by the binder solution. Furthermore, in the 3D printed  $Cu$  green samples, all the  $Cu$  particles were found to be properly interconnected and surrounded by binder. Thus, it could be inferred that high loading  $Cu$  ink is suitable for the DIW 3D printing process.

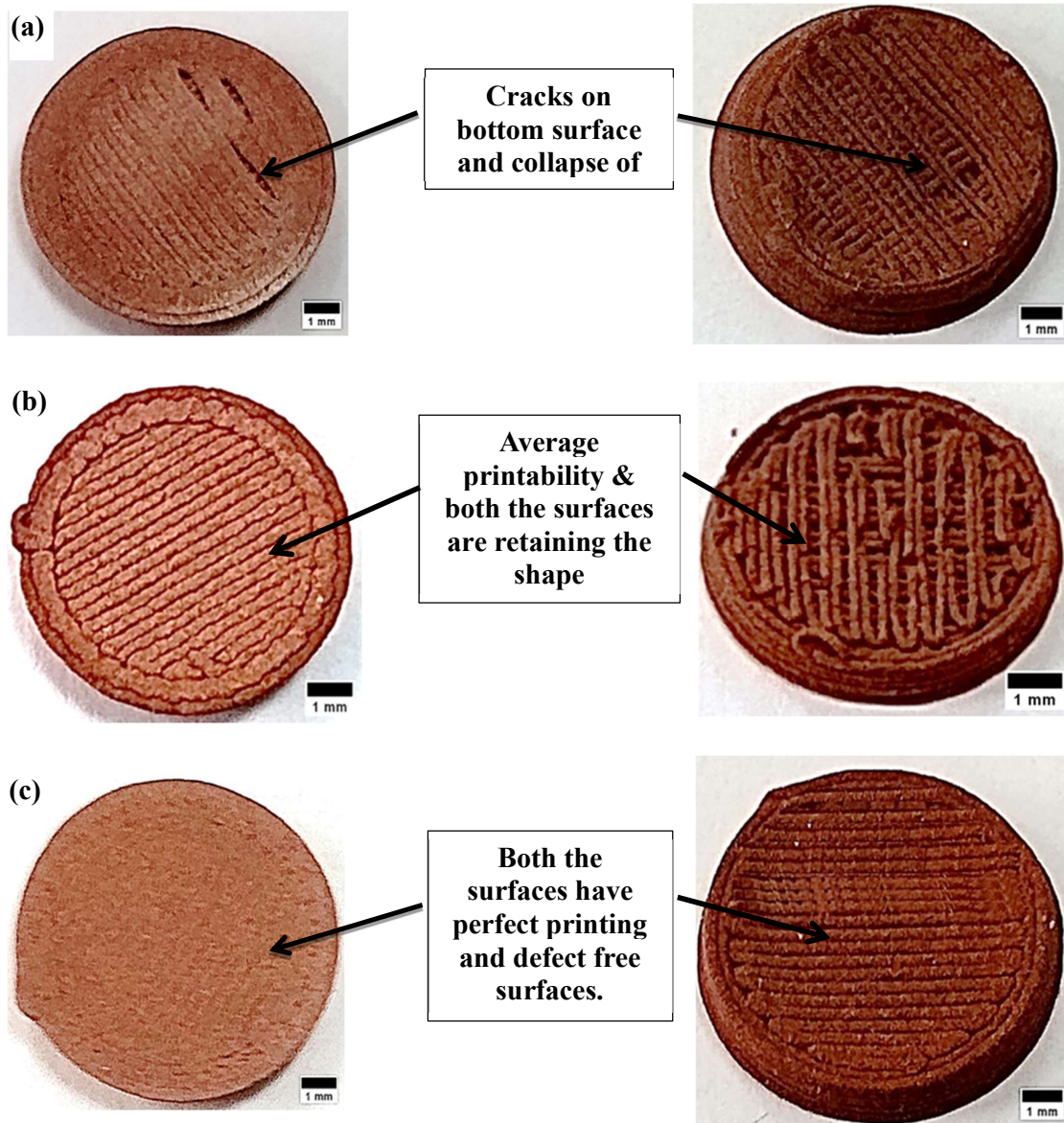


Fig. 4.5: Printed Green samples with a) 93 wt% b) 95 wt% c) 97 wt% Cu loading

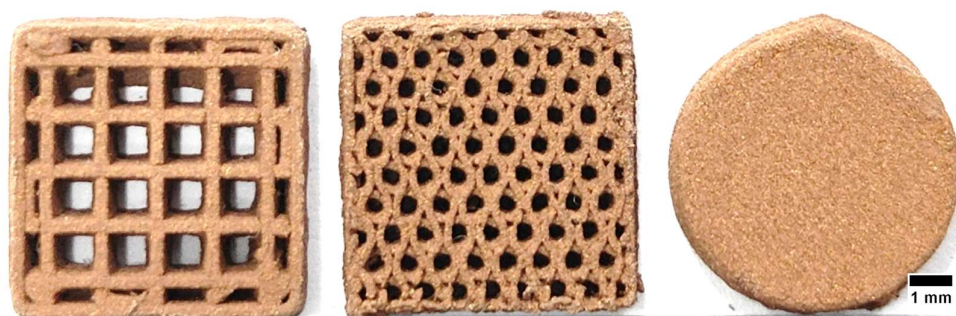


Fig. 4.6: Printed Green samples with 97 wt % Cu loading with Rectangular Mesh; Honeycomb structure and Cylinder

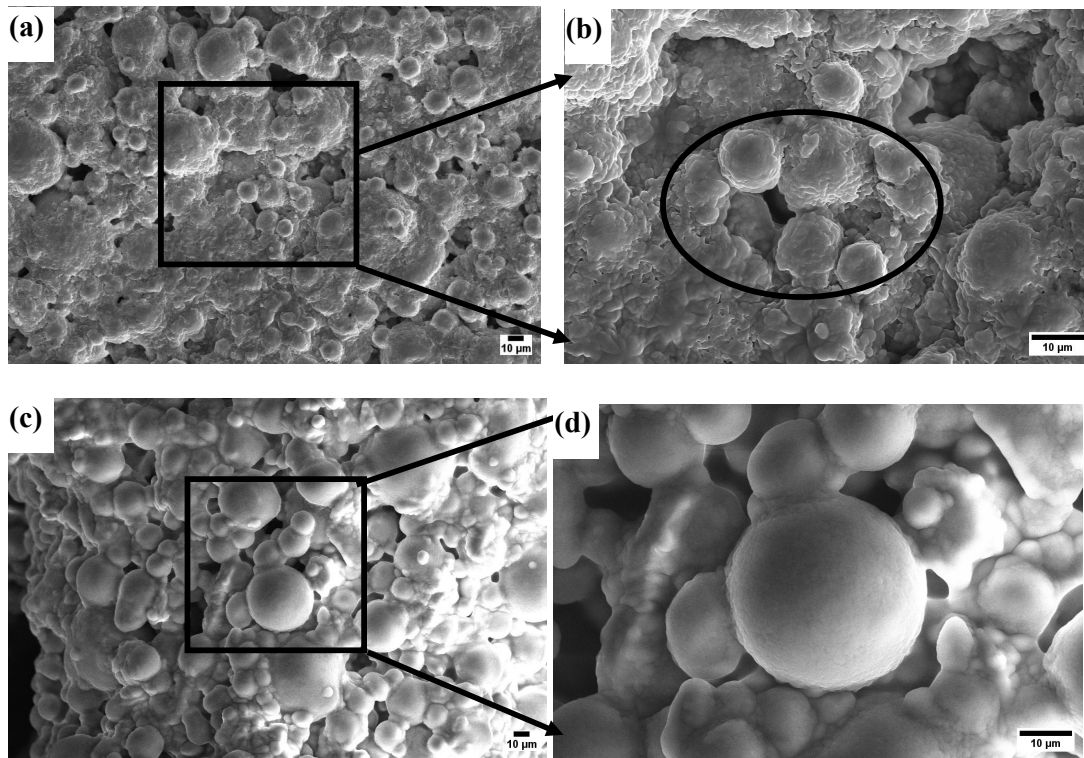


Fig. 4.7: SEM image of a, b ) Prepared ink with 97 wt% *Cu* loading & c, d) Green samples printed with 97 wt% *Cu* loading

#### 4.1.5 Morphological Characterization

All the samples were sintered at a sintering temperature of 980 °C with a heating rate 4 °C/min and soaking time of 3 h as reported in previous study [24]. Figures 4.8 (a) and (b) show the variation of sintered density and volumetric shrinkage with *Cu* loading.

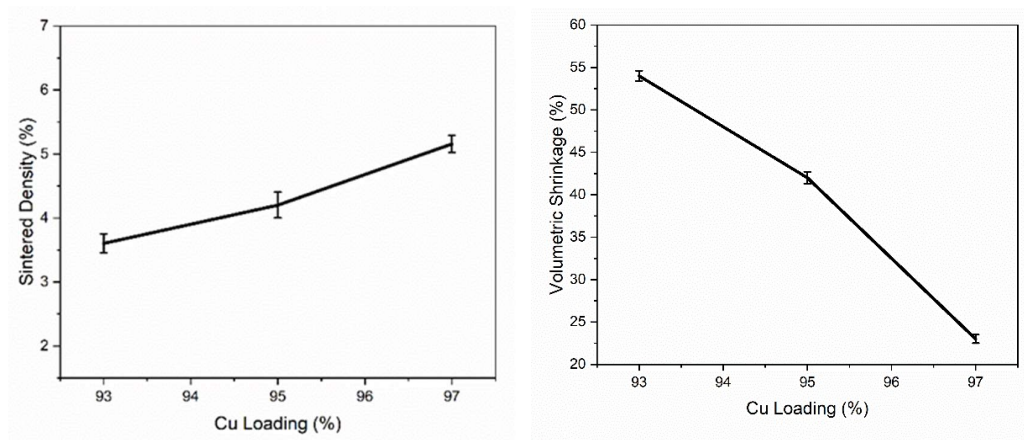


Fig. 4.8: Variations of volumetric shrinkage and sintered density with *Cu* loading

Table 4.2 provides the sintered density for all the samples prepared using 93 wt %, 95 wt % and 97 wt % Cu loading. As presented in Table 4.2, the highest sintered density was achieved in the sample prepared using the ink formulation with 97 wt% Cu loading. This observation is further supported by the trend shown in Fig. 4.8, which clearly demonstrates that with an increase in Cu particle content, there is a corresponding increase in the final sintered density and a noticeable decrease in volumetric shrinkage.

**Table 4.2 Sintered Cu sample density with 93 wt%, 95 wt% and 97 wt% loading**

<b>Sample category with Cu loading</b>	<b>Sample id</b>	<b>Direct measurement (<math>\rho</math>) g/cm<sup>3</sup></b>	<b>Archimedes measurement (<math>\rho</math>) g/cm<sup>3</sup></b>	<b>Average density g/cm<sup>3</sup></b>
Green / 97 wt% Cu Loading	1	4.313	4.241	4.314
	2	4.431	4.342	
	3	4.135	4.426	
Sintered / 97 wt% Cu loading	1	5.163	5.089	5.156
	2	5.209	5.210	
	3	4.956	5.311	
Green/95 wt% Cu loading	1	3.532	3.507	3.501
	2	3.646	3.484	
	3	3.315	3.529	
Sintered/95 wt% Cu loading	1	4.238	4.208	4.202
	2	4.375	4.181	
	3	3.978	4.235	
Green/93 wt% Cu loading	1	3.041	3.065	3.001
	2	3.184	2.878	
	3	2.806	3.029	
Sintered/ 93 wt% cu loading	1	3.648	3.678	3.604
	2	3.820	3.454	
	3	3.367	3.655	

This behavior can be explained by considering the composition of the ink and the role of the binder. In lower *Cu*-loaded inks, such as the 93 *wt%* formulation, a higher proportion of the binder is required to maintain the flowability and printability of the ink. During the sintering process, the binder is removed, leaving behind voids that contribute to greater shrinkage and lower final density. In contrast, the ink with 97 *wt%* *Cu* content contains a significantly reduced amount of binder and a much higher volume of metal particles.

Furthermore, the effect of variation in *Cu* and binder loading on the porosity of the sintered sample can be seen using the SEM images shown in Fig. 4.9.

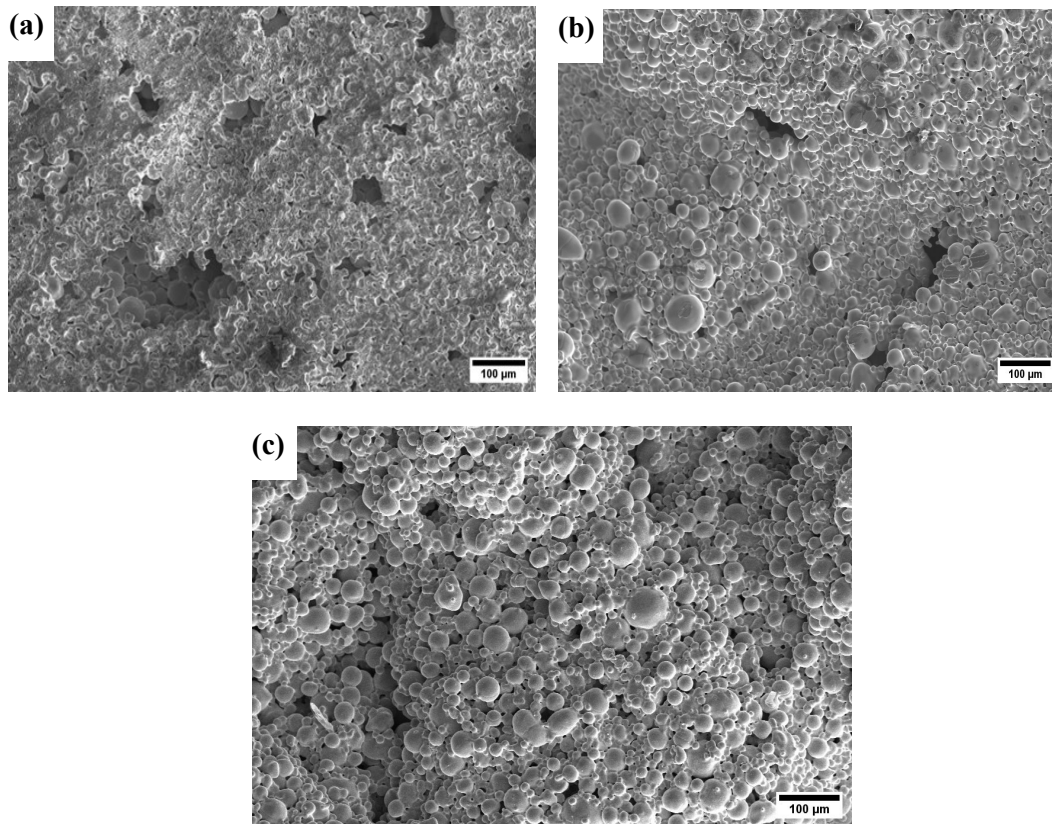


Fig.4.9: Micrograph of a) 93 *wt%* b) 95 *wt%* and c) 97 *wt%* *Cu* loaded sintered sample

It could be observed from Fig. 4.9 (a) that the sintered *Cu* sample prepared using 93 *wt%* *Cu* ink contains too many large-sized pores. For the 95% *Cu*-loaded sintered sample shown in Fig. 4.9 (b), fewer pores as compared to the 93 % *Cu*-loaded sample were observed. As compared to the 93 *wt%* and 95 *wt%* *Cu*-loaded sintered samples, the sample

prepared using 97% *Cu*-loaded ink exhibited a lesser number of pores. Also, the size of pores seen in 97% *Cu* samples was comparatively smaller as compared to the other two cases.

The large pore sizes in the 93 wt% and 95 wt% *Cu*-loaded samples signify the variation in the presence of binder content at different locations. The binder connection at some locations were higher as compared to other locations within the sample. The places where the binder amount was very much high, increases the porosity to a large extent. Moreover, a high amount of binder content will also distort the structure and reduce the mechanical strength. Hence, from the characterization of green and sintered *Cu* samples, it could be established that *Cu* ink having 97 wt% *Cu* loading was found to be optimum exhibiting ideal characteristics for both DIW 3D printing and sintering.

Thus, using 97% *Cu* ink, porous samples were fabricated. Thus, the prepared optimum *Cu* ink for DIW 3D printing was found suitable for the preparation of HP-*Cu* samples. The successful fabrication of precise printed parts relies not only on the development of an ideal ink but also on the careful optimization of printing parameters. While a well-formulated ink may possess desirable properties such as appropriate viscosity, stability, and particle dispersion, these alone are insufficient to ensure high-quality prints. Printing parameters, such as nozzle diameter, extrusion pressure, print speed, and layer height, directly influence ink flow behavior, layer adhesion, and geometric accuracy. The interaction between ink rheology and the process parameters in DIW is a highly coupled and complex relationship that plays a critical role in determining the quality, fidelity, and performance of the final printed structures. Ink rheology, which encompasses properties such as viscosity, yield stress, shear thinning behavior, and thixotropy, governs the flow behavior of the ink during extrusion, as well as its ability to retain shape after deposition. On the other hand, process

settings such as extrusion pressure, nozzle diameter, printing speed, layer height, and ambient conditions directly influence the ink's response during the printing process.

Even if an ink is perfectly formulated in terms of particle dispersion, binder concentration, and rheological properties, inappropriate selection of printing parameters can lead to several types of defects. These include nozzle clogging, filament breakage, dimensional inaccuracy, deformation, and poor surface finish. For instance, a low-viscosity ink may flow too freely under high pressure, resulting in spreading and loss of shape fidelity, whereas a high-viscosity ink may require excessive pressure to extrude, increasing the risk of clogging or inconsistent flow. Similarly, a mismatch between printing speed and extrusion rate can cause over-deposition or under-deposition, affecting the structural integrity and accuracy of the printed part.

Hence, the development of high-resolution, reliable, and functional structures via DIW mandates a finely balanced, synergistic optimization of both the ink formulation and the printing parameters. This involves not only tailoring the rheological behavior of the ink to suit the physical requirements of the printing process but also adapting the process settings in accordance with the ink's flow characteristics.

In the subsequent chapter, a detailed discussion will be presented on how various rheological attributes of the ink were systematically optimized in conjunction with key DIW parameters to realize defect-free, high-density, and geometrically accurate printed copper structures.